2015 IEEE/RSJ International Conference on Intelligent Robots and Systems (IROS)
Congress Center Hamburg
Sept 28 - Oct 2, 2015. Hamburg, Germany

Real-time Adaptive Kinematic Model Estimation of Concentric Tube Robots

Chunwoo Kim, Seok Chang Ryu and Pierre E. Dupont

***Abstract*— Kinematic models of concentric tube robots have matured from considering only tube bending to considering tube twisting as well as external loading. While these models have been demonstrated to approximate actual behavior, modeling error can be significant for medical applications that often call for positioning accuracy of 1-2mm. As an alternative to moving to more complex models, this paper proposes using sensing to adaptively update model parameters during robot operation. Advantages of this method are that the model is constantly tuning itself to provide high accuracy in the region of the workspace where it is currently operating. It also adapts automatically to changes in robot shape and compliance associated with the insertion and removal of tools through its lumen. As an initial exploration of this approach, a recursive on-line estimator is proposed and evaluated experimentally.**

I. Introduction

Concentric tube robots are a promising continuum robot technology that are being applied to a broad variety of interventions in such fields as neurosurgery [1], [2] and cardiac surgery [3], [4]. Comprised of a telescoping combination of precurved superelastic tubes, the shape of these robots is controlled by rotating and translating each tube with respect to the others at their base. Many aspects of this technology have been investigated including kinematic modeling [5]–[7], design and workspace evaluation [8]–[10], stability [11]–[13] and motion planning [14].

A continuing challenge, however, is that the most frequently used kinematic model [5], [6], while formulated from principles of mechanics, is a function of a small number of imprecisely known parameters. Furthermore, as designers of these robots attempt increasingly challenging applications, simplifying assumptions inherent in the model are being violated. For example, while the assumption of linear elasticity typically holds up to about 1% strain for NiTi [15], designs fabricated by our group often use significantly higher strains. Additional factors such as cross section ovalization and friction also contribute to model error.

Furthermore, the kinematic model can be time varying. Many procedures require the insertion and removal of tools and implants through the lumen of the robot. See, e.g., [3], [4]. As shown in Fig. 1(a), these devices are mounted at the tips of tubes that are inserted from the base of the robot. While designed to be compliant, these tubes change both the curvature and the compliance of the robot when inserted or removed. An additional source of model variation with time corresponds to relaxation of tube precurvature with use.

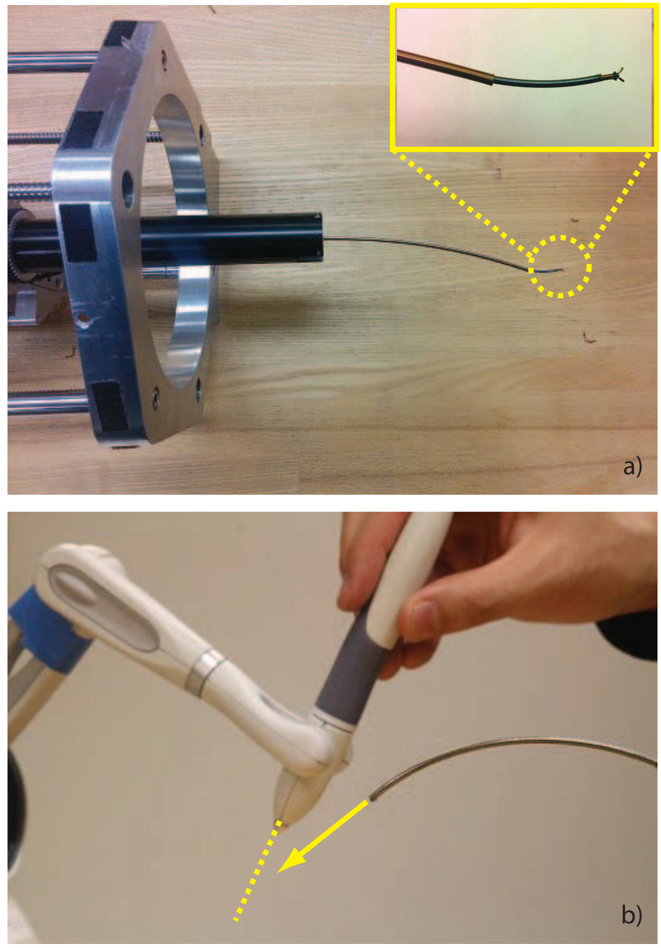

Fig. 1. Motivation for adaptive modeling. (a) Model perturbation due to insertion and removal of tools. (b) Mismatch in master and slave configurations due to model error.

Modeling error manifests as steady-state position or force error during closed-loop control. For example, most current implementations of tip position control for concentric tube robots are kinematic-model-based feedforward controllers [5]–[7]. During teleoperation, the operator manually closes a feedback loop by observing slave error and then moving the master beyond the desired position and orientation in order to drive the slave to the desired configuration. This can result in a confusing mismatch of configuration between master and slave as shown in Fig. 1(b).

The addition of a sensor-based feedback loop can improve

This work was supported by the National Institutes of Health under grant R01HL124020.

The authors are with the Department of Cardiovascular Surgery, Boston Children's Hospital, Harvard Medical School, Boston, MA 02115, USA
firstname.lastname@childrens.harvard.edu

978-1-4799-9994-1/15/$31.00 ©2015 IEEE

performance [16], [17], but is currently challenging to implement in practice since existing sensors, e.g., electromagnetic, tend to fill the entire robot lumen leaving no room for tools. As better sensors become available, the smoothest, most accurate motions will result from the combination of an accurate model-based feedforward controller with sensor-based feedback.

Several approaches to reducing model error are possible. The first is to derive more sophisticated models that incorporate some combination of neglected phenomena. This approach will help the community sort through the relative importance of the various effects. This will, however, add to the complexity of solving the equations in real time. Furthermore, the insertion and removal of additional tubes for tool delivery is an important case. And, while this can be certainly modeled analytically, it is impossible to predict what tube or tube shape a clinician may attempt to insert through a robot in an actual procedure.

These observations motivate an alternative approach, which is to use existing models, but to adaptively update the model parameters. This approach, while requiring sensing, provides several advantages. For example, the model can automatically adapt to changes associated with the insertion and removal of tool tubes. Furthermore, the parameters of a kinematic model are typically calibrated to minimize error over the entire workspace of a robot. Many surgical procedures, however, are confined to small regions of the workspace. Adaptive tuning of model parameters within these regions at the start of a procedure can enable substantial local error reduction. It is always possible to save both the global parameter values as well as parameters tuned for different workspace regions in order to facilitate transitioning outside the current region.

Considering tip position control, the sensing required for model adaptation could be provided by electromagnetic tracking [16], [17], FBG curvature sensing [18] or by imaging [19], [20]. Most of these sensors have a separate coordinate system that must be registered to the robot coordinate system. Another advantage of model adaptation is that the registration transformation can be incorporated into the kinematic model and included in the online adaptation.

On-line model estimation and adaptive control have been considered extensively for rigid robots. See, e.g., [21]–[23]. Much of this work exploits the fact that the kinematic and dynamic equations of rigid manipulators are linear in terms of the link parameters, which is not generally the case for continuum robots.

In the context of tendon-based continuum robots, a few papers have considered adaptive modeling [24], [25]. For example, in [24], recursive linear estimation is used to update friction and backlash parameters for actuation compensation. In [25], the authors propose a technique called model-less control in which the kinematic Jacobian is continuously estimated based on commanded differential motions of the actuators and sensed tip location - without using a nominal underlying kinematic model. In an alternative approach, Gaussian Process Regression was used to learn an unknown function that modifies the control input to compensate for the imprecise internal kinematics model of a cable-driven surgical assistant robot [26].

The contribution of this paper is to propose, develop and validate a method for on-line adaptive kinematic modeling of concentric tube robots. This approach can provide some of the robustness to disturbances addressed by model-less control while still providing the real-time error reduction associated with accurate feedforward control. Section II summarizes the current mechanics-based model as well as the functional approximation described in [5]. This section also describes a recursive approach to parameter estimation. This section also describes a recursive approach to parameter estimation. Validation experiments appear in Section III and conclusions in Section IV.

II. Kinematic Modeling

Mechanics models of concentric tube robots have been developed [5]–[7] under certain assumptions: tubes can bend and twist elastically, but cross section shear and axial elongation are neglected. Furthermore, tube stiffness in bending and torsion is assumed to be linear elastic.

While this model and parameter set are very useful for designing a tube set with a desired workspace [12], it ignores phenomena such as friction [27] as well as nonlinear elastic material behavior. Thus, it can be anticipated that when the parameters are calibrated over the entire workspace, it will be impossible to eliminate error due to these unmodeled phenomena.

To avoid the real-time computational burden of solving this split boundary value problem, an algebraic functional approximation was previously proposed [5]. In this approach, the mechanics model was solved off line for a dense set of tip configurations over the workspace. The input-output data pairs of actuator variables (tube rotations and extensions) and tip configurations were then modeled using a product of truncated Fourier series. For example, a positional coordinate, $p_i(s_{\max})$ was represented by

$$p_i(s_{\max}) = \left(\prod_{j=2}^{n} H(\alpha_j, q)\right)\left(\prod_{k=2}^{n} H(L_k/\lambda_k, q)\right) \quad (1)$$

$$H(\beta_j, q) = \sum_{k=-q}^{+q} c_k e^{i(k\beta_j)} \quad (2)$$

Here, $H(\beta_j, q)$ is a scalar Fourier series of order q involving the actuator variable β_j. The first product term in (1) involves the rotational inputs while the second term involves tube extension variables, L_k, nondimensionalized using wavelength parameters λ_k.

Using this representation, the forward kinematic solution reduces to an algebraic function evaluation while the inverse kinematic solution was implemented as a root finding problem. The order of the Fourier series, q, determines the number of free parameters of the model and can be selected to achieve a desired maximum error over the workspace. Assuming the same order series for all actuator variables and that each tube is rotated and translated independently, each tip coordinate is modeled by $(2n-1)(2q+1)$ parameters.

While the model was originally validated based on its ability to closely match the input/output data of the mechanics-based model, an additional unintended benefit of this approach is that the adjustable number of model parameters may enhance the ability of the model to match the actual kinematics.

An additional advantage is that the model is linear in its parameters and so, for example, positional coordinate $p_i(s_{\max})$ can be written as

$$p_i(s_{\max}) = \bar{c}^T_{p_i(s_{\max})} \bar{\phi}(\alpha_2, \ldots, \alpha_n; L_2, \ldots, L_n) \qquad (3)$$

where $\bar{c}_{p_i(s_{\max})} \in \Re^{(2n-1)(2q+1)}$ is a vector obtained by appropriately stacking the Fourier coefficients in (1) and $\bar{\phi}$ is the vector of corresponding trigonometric terms. Thus, it is possible to refine parameter values on line using recursive least squares as described in the subsection below.

A. Recursive Algebraic Model Estimation

Recursive least square (RLS) [28] is an algorithm to recursively update the parameters of a linear model from the observed output. This algorithm was chosen as it is straightforward to implement on the functional approximation kinematics model and is linear in its parameters. The updated parameter set is optimal in the sense that it minimizes the weighted sum of squares of the error between the observed and predicted output. In terms of the parameter $\bar{c}$ and measured position coordinates p of (3), the estimated parameter $\bar{c}_{k+1}$ from the k observation is given by

$$\bar{c}_{k+1} = \arg\min_{\bar{c}} \sum_{i=1}^{k} \kappa^{k-i} |\bar{c}^T \bar{\phi}_i - p_i|^2 \qquad (4)$$

The weighting factor $\kappa \leq 1$ is called a "forgetting factor" since it assigns less weight to earlier errors. Instead of solving the optimization problem of (4), $\bar{c}_{k+1}$ can be recursively updated from its value $\bar{c}_k$ at the previous step and the k^{th} measured position coordinates, p_k, by the following equations.

$$\varepsilon_k = p_k - \bar{c}_k^T \bar{\phi}_k \qquad (5)$$

$$M_{k+1} = \frac{1}{\kappa}\left(M_k - \frac{1}{\kappa + \bar{\phi}_k^T M_k \bar{\phi}_k} M_k \bar{\phi}_k \bar{\phi}_k^T M_k \right) \qquad (6)$$

$$\bar{c}_{k+1} = \bar{c}_k + \varepsilon_k M_{k+1} \bar{c}_k \qquad (7)$$

There are two free parameters that can be tuned and influence the performance of the on-line parameter estimation. One is the the initial value of the matrix M_0 and the other is the forgetting factor κ. The matrix M is related to the covariance of the kinematics input $\bar{\phi}$. Its initial value, M_0, can be estimated from the sampled kinematics inputs collected prior to adaptation or it can be initialized to an identity matrix multiplied by constant, $M_0 = \sigma I$ [28]. The initial value can significantly impact the rate of convergence.

Since it has not been shown that the actual kinematic model lies in the set of models corresponding to the algebraic model, it is likely that the best fit parameters of the algebraic model will vary for different regions of the workspace. Consequently, selection of the forgetting factor, which controls the contribution of prior prediction errors to the parameter update, may have significant implications when moving between regions of the workspace. The choice of forgetting factor is a compromise between local tracking accuracy, speed of response to perturbations and stability [29].

III. Experiments

The proposed adaptive estimation method was evaluated using the teleoperated concentric tube robot depicted in Fig. 2a. Due to space limitations, only adaptation of the position coordinates is considered here. The robot is comprised of three tubes with parameters listed in Table I where regions of constant curvature are denoted by section number. The two outer tubes form a variable curvature section and are rotated independently, but translated together. The innermost tube is significantly more compliant that the outer two tubes and is translated and rotated independently of the other tubes. Thus, the kinematic variables are $\{\alpha_2, \alpha_3, L_3\}$. Including translation and rotation of the tube assembly, the robot possesses five degrees of freedom. The missing degree of freedom is the roll orientation at the tip.

The robot controller was implemented on a PC in C++ using a CAN bus to communicate velocity commands to each motor amplifier. Desired tip position and orientation are read from the encoders of a 6 DOF haptic interface (Phantom Omni) and converted to motor commands by computing the inverse kinematic solution using a second-order model based on (2). The model has 125 parameters per tip coordinate which were initialized by pre-computing 40 x 40 x 40 grid points over the workspace using measured values of tube stiffness, curvature and length.

The controller block diagram is shown in Fig. 3. A motor-control loop operates via the CAN bus at 1Mbps, reading motor counts and sending velocity commands. The teleoperation loop operates at 1kHz reading commands from the haptic device, computing the inverse kinematics using root finding and updating the set point for the motor controller. The adaptive model estimator runs at 240Hz reading the position of the robot tip from an electromagnetic (EM) sensor and updating the kinematic model.

An EM tracker sensor (TrackStar, NDI, Waterloo, Canada) was mounted at the tip of the robot to track tip position and orientation and was integrated with an adaptive parameter estimator as shown in Fig. 3. The robot was registered to the sensor coordinate system by rotating the entire tube set around the its axis (Z in Fig. 2b) and then fitting a circle to the measured position of the tip. When the robot is in its initial configuration, the initial position of the tip in the robot coordinate system is $(r, 0, d)$, as shown in Fig. 2b. Then, when the tube set is rotated, the measured tip position forms a circle of radius r on a plane Z=d with center located at

TABLE I
CONCENTRIC TUBE PARAMETERS.

	Tube 1	Tube 2	Tube 3	
	Section 1	Section 1	Section 1	Section 2
Length (mm)	150	150	150	86.39
Curvature (m^{-1})	4.348	4.348	0.0	18.182
Relative Stiffness	1	1	0.286	0.286

$(0,0,d)$ in the robot coordinate system. Fitting a circle to the measured tip positions identifies the plane and the center of the circle. The Z and X axes of the robot coordinate system comprise the normal of the circle and the line from the circle center to the initial tip position, respectively. The origin of the robot coordinate system is located $d$mm away from the center along Z axis. The value of the parameter d is measured from the tube design.

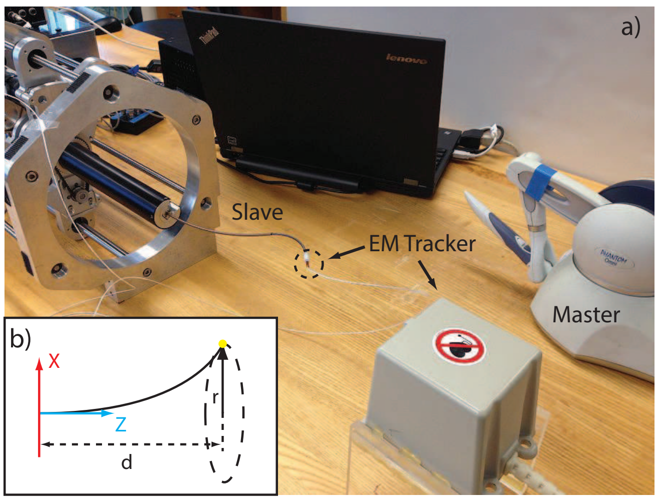

Fig. 2. a) Teleoperated concentric tube robot. b) Coordinate system of the CTR used for registration.

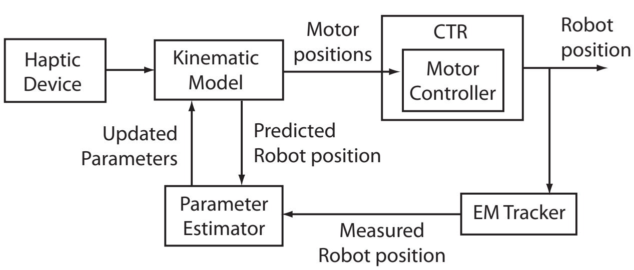

Fig. 3. Control and model estimation block diagram.

To validate the proposed approach, two types of experiments were conducted. The first considered model adaptation for motions performed in a specific region of the workspace. This is intended to reproduce the situation in which a surgery will involve precise motions in a localized region. The second type of experiment addresses model adaptation when a tool is first inserted and then removed from the robot lumen.

In these experiments, the matrix M of the recursive least square estimation was initialized as $M_0 = \sigma I$, with $\sigma = 0.1$. The value of σ influenced the convergence speed of the adaptation and the errors during the adaptation. This value was found to provide fast convergence and was used for all experiments. The forgetting factor κ was set to unity leading to equal weighting of the entire measurement history. This is a reasonable choice for trajectories located in one region and represents the conservative limit of what can be achieved through adaptation.

A. Trajectory-based Model Adaptation

To evaluate adaptation in a specific region of the workspace, a periodic trajectory was generated corresponding to the robot tip tracing a square in space. The square was 40mm on a side, was perpendicular to the z axis and was centered at $\{0,0,210\}$. The desired tip orientation was specified as the constant value of $\{0,0,1\}$. The robot was commanded to trace out the square at a speed of 16mm/s.

Initially, model-adaptation was turned off and the error shown in Fig. 4(a) reflects the difference between actual robot kinematics and the algebraic model whose parameters have been fit to the mechanics-based model. Note that registration error could also be present here and would correspond to a rigid body displacement.

The adaptive estimator was then turned on and allowed to update the model as the square trajectory was traversed five times. The five traversals are plotted in Fig. 4(b). Notice that convergence to a steady-state path occurs almost immediately. To quantitatively examine convergence, the path error magnitude as a function of time is plotted in Fig. 5 with and without adaptation. Without adaptation, the error is a constant periodic function with a maximum error of 8mm, but with adaptation, maximum error over the perimeter never exceeds 3mm.

To examine the error from a geometric perspective, its in-plane and out-of-plane components are plotted in Fig. 6 as a function of perimeter coordinate. Again, notice that error reduction occurs so quickly that the transient is not visible.

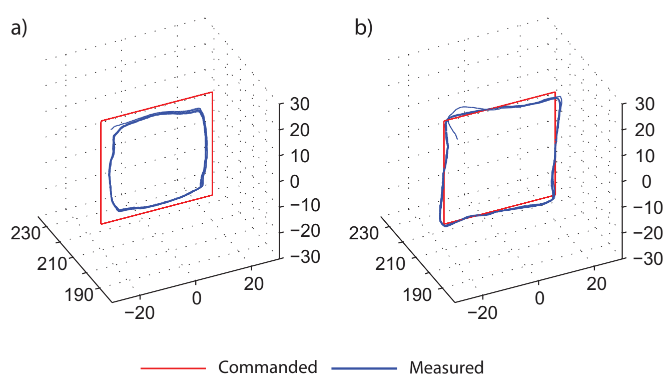

Fig. 4. Trajectory tracking results. (a) No adaptation. (b) With adaptation.

B. Robustness to Tool Insertion and Removal

To evaluate the ability of the method to adapt to model perturbations caused, e.g., by the insertion and removal of tools through the robot lumen, additional experiments were

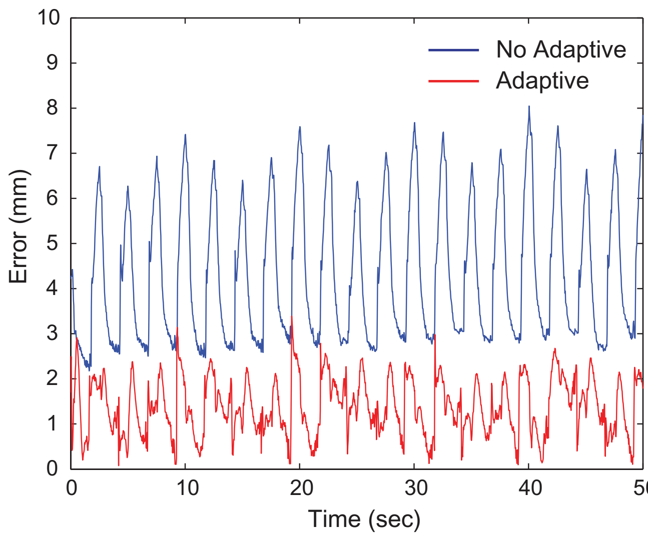

Fig. 5. Total path error versus time for square trajectory.

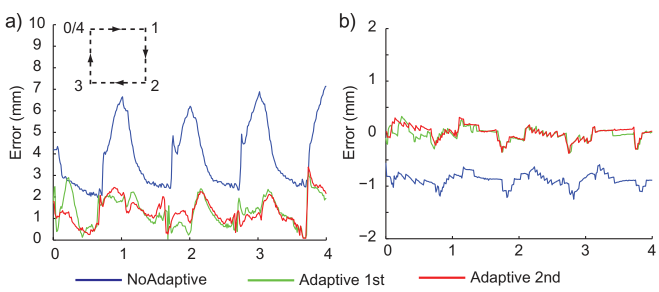

Fig. 6. Parameterized path error versus perimeter coordinate. (a) In-plane error. (b) Out-of-plane error.

performed. To simulate tool delivery, a 0.8mm NiTi wire inserted inside a 1.45mm outer diameter polyimide tube was used. This combination is similar to the system used to delivery and actuate the forceps shown in Fig. 1(a).

For these experiments, the robot tip was commanded to trace out a 40mm diameter circle at a velocity of 14mm/sec (40°/s). The circle was normal to the x axis and centered at $\{-35,0,180\}$. The desired tip orientation was specified as the constant value of $\{-\sin 60°, 0, \cos 60°\}$. In initial tests with this trajectory, it was observed that minimum error was achieved in 2 traversals of the circle. Consequently, results reported below correspond to those achieved after 2 adaptive traversals of the curve. Error distance is reported using a parameterization of in-plane radial distance, e_r, and out-of-plane distance, e_p.

The ability to adapt to a model change due to tool insertion and removal is illustrated Fig.7. Fig.7(a) illustrates initial model error prior to any adaptive tuning and prior to tool insertion (maximum error: $e_r = 6.42$mm, $e_p = 5.41$mm). The adaptive algorithm is then turned on and run for 2 traversals resulting in the converged path of Fig.7(b) (maximum error: $e_r = 1.37$mm, $e_p = 1.66$mm).

The adaptive algorithm was then turned off and the mock tool was next inserted in the robot lumen. The effect of

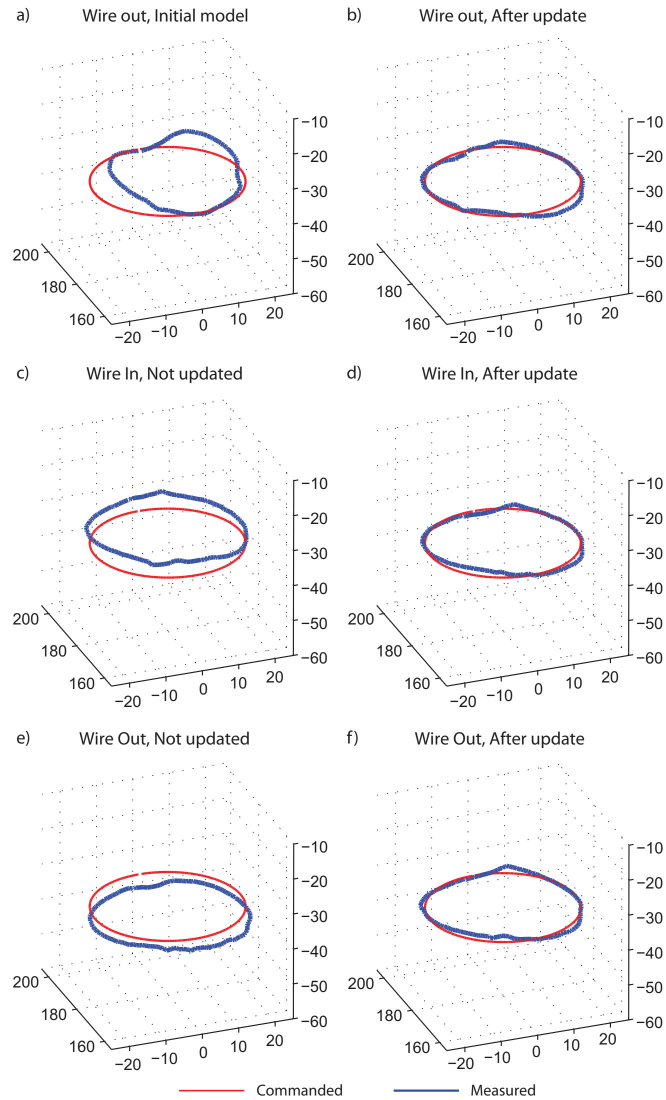

Fig. 7. Circular trajectory tracking a) using initial kinematic model, b) after adaptive update, c) using same model from b) after insertion of tool tube, d) with model updated to compensate for tool insertion, e) using same model from d) after removing tool tube, and f) with model updated to compensate for tool tube removal.

inserting the straight tube and wire is to straighten the robot causing the path shown in Fig.7(c) to rise roughly vertically above the commanded path (maximum error: $e_r = 2.94$mm, $e_p = 3.93$mm). Allowing the adaptive algorithm to run for 2 traversals, however, eliminates much of this perturbation as shown in Fig.7(d) (maximum error: $e_r = 1.61$mm, $e_p = 1.34$mm).

When adaptation is turned off and the straight tube and wire are removed, robot curvature increases causing the path to shift downward as shown in Fig.7(e) (maximum error: $e_r = 2.04$mm, $e_p = 3.49$mm). Finally, adaptation is turned back on and the model converges again to the desired circle as shown in Fig.7(f) (maximum error: $e_r = 1.52$mm, $e_p = 1.97$mm).

IV. CONCLUSIONS

This paper proposes a new direction in the control of concentric tube robots, namely, adaptive on-line model estimation. There are many reasons why such algorithms could prove to be an important component of any commercial concentric tube robot control system. For example, small variations in the geometric and mechanical properties of tube sets comprising any robot design will likely necessitate initial calibration of every tube set. Furthermore, significant modeling error can occur during operation due to both neglected mechanical phenomena (e.g., nonlinear elasticity) and perturbations, such as tool insertion and removal.

The approach described here exploits the linearity with respect to model parameters of the kinematic functional approximation proposed in [5]. This enables model adaptation to be implemented using recursive least squares. By selecting the order of Fourier series used in the functional approximation, this approach also provides a direct means to control the number of free parameters of the kinematic model.

REFERENCES

[1] V. P. Bodani, H. Azimian, T. Looi, and J. M. Drake, "104 design and evaluation of a concentric tube robot for minimally-invasive endoscopic pediatric neurosurgery." *Neurosurgery*, vol. 61, p. 192, 2014.

[2] P. J. Swaney, H. B. Gilbert, R. J. Webster III, P. T. Russell III, and K. D. Weaver, "Endonasal Skull Base Tumor Removal Using Concentric Tube Continuum Robots: A Phantom Study," *Journal of Neurological Surgery Part B: Skull Base*, In Press.

[3] N. V. Vasilyev, A. H. Gosline, E. Butler, N. Lang, P. J. Codd, H. Yamauchi, E. N. Feins, C. R. Folk, A. L. Cohen, R. Chen, D. Zurakowski, P. J. del Nido, and P. E. Dupont, "Percutaneous steerable robotic tool delivery platform and metal microelectromechanical systems device for tissue manipulation and approximation: Closure of patent foramen ovale in an animal model," vol. 6, no. 4, pp. 468–475, 2013.

[4] N. V. Vasilyev, A. H. Gosline, A. Veeramani, M. T. Wu, G. P. Schmitz, R. T. Chen, V. Arabagi, P. J. del Nido, and P. E. Dupont, "Tissue removal inside the beating heart using a robotically delivered metal mems tool," vol. 34, no. 2, pp. 236–247, 2015.

[5] P. Dupont, J. Lock, B. Itkowitz, and E. Butler, "Design and control of concentric-tube robots," *Robotics, IEEE Transactions on*, vol. 26, no. 2, pp. 209–225, April 2010.

[6] D. C. Rucker, R. J. Webster, G. S. Chirikjian, and N. J. Cowan, "Equilibrium conformations of concentric-tube continuum robots," *The International Journal of Robotics Research*, 2010.

[7] R. Xu, A. Asadian, A. Naidu, and R. Patel, "Position control of concentric-tube continuum robots using a modified jacobian-based approach," in *Robotics and Automation (ICRA), 2013 IEEE International Conference on*, May 2013, pp. 5813–5818.

[8] C. Bedell, J. Lock, A. Gosline, and P. Dupont, "Design optimization of concentric tube robots based on task and anatomical constraints," in *Robotics and Automation (ICRA), 2011 IEEE International Conference on*, May 2011, pp. 398–403.

[9] T. Anor, J. Madsen, and P. Dupont, "Algorithms for design of continuum robots using the concentric tubes approach: A neurosurgical example," in *Robotics and Automation (ICRA), 2011 IEEE International Conference on*, May 2011, pp. 667–673.

[10] J. Burgner-Kahrs, H. Gilbert, J. Granna, P. Swaney, and R. Webster, "Workspace characterization for concentric tube continuum robots," in *Intelligent Robots and Systems (IROS 2014), 2014 IEEE/RSJ International Conference on*, Sept 2014, pp. 1269–1275.

[11] R. J. Webster III, J. M. Romano, and N. J. Cowan, "Mechanics of Precurved-Tube Continuum Robots," *IEEE Transactions on Robotics*, vol. 25, no. 1, pp. 67–78, 2009.

[12] C. Bergeles, A. Gosline, N. Vasilyev, P. Codd, P. del Nido, and P. Dupont, "Concentric tube robot design and optimization based on task and anatomical constraints," *Robotics, IEEE Transactions on*, vol. 31, no. 1, pp. 67–84, Feb 2015.

[13] J. Ha, F. Park, and P. Dupont, "Achieving elastic stability of concentric tube robots through optimization of tube precurvature," in *Intelligent Robots and Systems (IROS 2014), 2014 IEEE/RSJ International Conference on*, Sept 2014, pp. 864–870.

[14] C. Bergeles and P. Dupont, "Planning stable paths for concentric tube robots," in *Intelligent Robots and Systems (IROS), 2013 IEEE/RSJ International Conference on*, Nov 2013, pp. 3077–3082.

[15] D. Stoeckel, "Nitinol medical devices and implants," *Minimally invasive therapy & allied technologies*, vol. 9, no. 2, pp. 81–88, 2000.

[16] M. Mahvash and P. Dupont, "Stiffness control of surgical continuum manipulators," *Robotics, IEEE Transactions on*, vol. 27, no. 2, pp. 334–345, April 2011.

[17] S. Patil, J. Burgner, R. Webster, and R. Alterovitz, "Needle steering in 3-d via rapid replanning," *Robotics, IEEE Transactions on*, vol. 30, no. 4, pp. 853–864, Aug 2014.

[18] S. C. Ryu and P. Dupont, "Fbg-based shape sensing tubes for continuum robots," in *Robotics and Automation (ICRA), 2014 IEEE International Conference on*, May 2014, pp. 3531–3537.

[19] E. Lobaton, J. Fu, L. Torres, and R. Alterovitz, "Continuous shape estimation of continuum robots using x-ray images," in *Robotics and Automation (ICRA), 2013 IEEE International Conference on*, May 2013, pp. 725–732.

[20] H. Ren and P. Dupont, "Tubular enhanced geodesic active contours for continuum robot detection using 3d ultrasound," in *Robotics and Automation (ICRA), 2012 IEEE International Conference on*, May 2012, pp. 2907–2912.

[21] J.-J. E. Slotine and W. Li, "On the adaptive control of robot manipulators," *The International Journal of Robotics Research*, vol. 6, no. 3, pp. 49–59, 1987.

[22] R. Ortega and M. W. Spong, "Adaptive motion control of rigid robots: A tutorial," *Automatica*, vol. 25, no. 6, pp. 877 – 888, 1989.

[23] C. C. Cheah, C. Liu, and J. J. E. Slotine, "Adaptive tracking control for robots with unknown kinematic and dynamic properties," *The International Journal of Robotics Research*, vol. 25, no. 3, pp. 283–296, 2006.

[24] K. Xu and N. Simaan, "Actuation compensation for flexible surgical snake-like robots with redundant remote actuation," in *Robotics and Automation, 2006. ICRA 2006. Proceedings 2006 IEEE International Conference on*, May 2006, pp. 4148–4154.

[25] M. Yip and D. Camarillo, "Model-less feedback control of continuum manipulators in constrained environments," *Robotics, IEEE Transactions on*, vol. 30, no. 4, pp. 880–889, Aug 2014.

[26] J. Mahler, S. Krishnan, M. Laskey, S. Sen, A. Murali, B. Kehoe, S. Patil, J. Wang, M. Franklin, P. Abbeel, and K. Goldberg, "Learning accurate kinematic control of cable-driven surgical robots using data cleaning and gaussian process regression," in *Automation Science and Engineering (CASE), 2014 IEEE International Conference on*, Aug 2014, pp. 532–539.

[27] J. Lock and P. Dupont, "Friction modeling in concentric tube robots," in *Robotics and Automation (ICRA), 2011 IEEE International Conference on*, May 2011, pp. 1139–1146.

[28] S. Haykin, *Adaptive Filter Theory (3rd Ed.)*. Upper Saddle River, NJ, USA: Prentice-Hall, Inc., 1996.

[29] C. Paleologu, J. Benesty, and S. Ciochina, "A robust variable forgetting factor recursive least-squares algorithm for system identification," *Signal Processing Letters, IEEE*, vol. 15, pp. 597–600, 2008.